

Preparation of TiO₂–ZrO₂ mixed oxides with controlled acid–basic properties

M.E. Manríquez^a, T. López^a, R. Gómez^{a,b,*}, J. Navarrete^b

^a *Depto. Química, Universidad Autónoma Metropolitana-Izt., A.P. 55-534, México D.F. 09340, Mexico*

^b *Instituto Mexicano del Petróleo, Lázaro Cárdenas 152, 07730 México D.F., Mexico*

Received 14 May 2004; received in revised form 3 June 2004; accepted 3 June 2004

Available online 17 July 2004

Abstract

Titania–zirconia mixed oxides with various ZrO₂ content in TiO₂ (10, 50 and 90 wt.%) were prepared by the sol–gel method. High specific surface areas (77–244 m²/g) were obtained. Acidity determined by NH₃-TPD and FTIR-pyridine adsorption showed that in mixed oxides the number of acid sites is dramatically increased; it varies from 173 μmol NH₃/g for TiO₂ to 1226–1456 μmol NH₃/g for the mixed oxides. FTIR-pyridine adsorption showed the presence of Lewis sites in the catalysts. Basic sites were identified by FTIR-CO₂ adsorption, suggesting the formation of mixed oxides with acid–basic properties. XRD spectra identified anatase in the TiO₂ rich region, amorphous material in the mixed oxide 50–50 TiO₂–ZrO₂ and tetragonal and monoclinic crystalline phases in the ZrO₂ rich region. Activity in the isopropanol decomposition showed a good correlation between the acid–basic properties and the selectivity to propene, acetone and isopropyl ether. The latter was found as a product which mainly depends of the acid sites density.

© 2004 Elsevier B.V. All rights reserved.

Keywords: Titania–zirconia sol–gel; XRD-TiO₂–ZrO₂; Isopropanol dehydration; Titania–zirconia acid–base properties; Titania–zirconia catalysts; Titania–zirconia FTIR; Titania–zirconia ammonia TPD

1. Introduction

Alcohols dehydration is an important catalytic test to identify acid and basic sites in heterogeneous catalysts [1,2]. To established strength, distribution and density of acid sites, alcohols decomposition has been carefully studied. Between them isopropanol [3,4], 1-butanol [5,6], and 4-methyl-2-pentanol dehydration [7,8] are the reactions most frequently reported. The main products for the 1-butanol dehydration are 1-butene and the corresponding isomerized olefins, the formation of dibutylether was also observed. For 4-methyl-2-pentanol dehydration, hexenes and skeletal rearrangements were reported as products; in this reaction the formation of ethers is not observed. On the other hand, in spite of the difficult to correlate the catalysts acidity with activity and selectivity, isopropanol decomposition is a recommendable reaction, since dehydration, dehydrogenation and condensation reactions simultaneously

occurs [9]. The analysis of the products distribution, propene, acetone and isopropylether, give helpful information to understand the role of the acidity strength, acid sites density and acid–basic properties of the catalysts [10–12].

Alcohols decomposition has been carried out in a large number of catalysts showing strong or medium acidity, like silicoaluminates or aluminas [13,14] in which the isopropylether selectivity in minor to 10%, in these catalysts propene is the major product. In catalysts with low acidity as ZrO₂ [15] or TiO₂ [16], and also in the so-called basic catalysts as MgO [17,18], the main products are propene or acetone and practically the formation of the ether is not observed.

Since selectivity in alcohols decomposition depends of the strength and distribution of the acid sites, efforts have recently made in order to design catalysts with controlled acidity, and mixed oxides were prepared with these purposes. However, by example in SiO₂–MgO [19] or ZrO₂–MgO [11] showing basic properties the ether formation is not observed in the isopropanol decomposition. On the other hand for the Al₂O₃–MgO acid–basic mixed oxides isopropyl ether is not obtained and the propene/acetone ratio strongly depends of the preparation conditions [19,20].

* Corresponding author. Tel.: +55 58044668; fax: +55 58044666.

E-mail address: gomr@xanum.uam.mx (R. Gómez).

Table 1
Experimental relationships used in the synthesis of the TiO₂–ZrO₂ mixed oxides

| TiO ₂ –ZrO ₂ weight ratio (wt.%) | Titanium butoxide (mol) | Zirconium butoxide (mol) |
|--|-------------------------|--------------------------|
| 10–90 | 0.05 | 0.29 |
| 50–50 | 0.25 | 0.17 |
| 90–10 | 0.45 | 0.03 |

In the present work TiO₂–ZrO₂ mixed oxides were synthesized by the sol–gel method and evaluated in the isopropanol decomposition. The purpose is to obtain catalysts showing acid and basic properties with high selectivity to the formation of ethers, additives in use to increase gasoline octane number. Nitrogen isotherms and X-ray diffraction (XRD) were used to characterize textural and structural properties of the solids. FTIR-pyridine adsorption and ammonia thermodesorption (TPD-NH₃) were used to evaluate acidity; the basicity was characterized by means of FTIR-CO₂ spectroscopy.

2. Experimental

The precursors employed in the preparation of the sol–gel catalysts were titanium *n*-butoxide (98%, Aldrich) and zirconium *n*-butoxide (99%, Aldrich) in *n*-butanol (Baker, 99%). Reference titania was prepared as follows: 3.0 mol of *n*-butanol was put in a glass system at low temperature (0 °C) with constant stirring. After, 0.5 mol of titanium *n*-butoxide were drop-wise added to the solution and then the pH was adjusted to 3.0 with HNO₃ (Baker 56 vol.%). The flask was put under reflux at 70 °C and stirred for 5 h. Finally 3.3 mol of H₂O were added to the reaction system and the resulting suspension was maintained under reflux and constant stirring until gelling was achieved. The ZrO₂ reference was synthesized in the same using way but zirconium *n*-butoxide as zirconia precursor.

TiO₂–ZrO₂ mixed oxides were synthesized following the above described procedure. Appropriate amounts of the titanium and zirconium alkoxides were simultaneously added drop by drop to the *n*-butanol solution at 0 °C and the pH was adjusted at 3.0 with nitric acid. Then the mixture was put in reflux at 70 °C, and the water for the hydrolysis was added. The amounts for the two alkoxides used for the different synthesis are reported in Table 1. After gelling the samples were dried under vacuum for 24 h at 70 °C. Finally the gels were annealed at 400 °C during 4 h in air.

3. Characterization

3.1. Specific surface area

Textural properties were determined from the nitrogen adsorption isotherms obtained with a Micromeritics ASAP

2000 automated apparatus. The specific surface areas were calculated from the isotherms using the BET method.

3.2. X-ray diffraction

Specimens were prepared packing the powder samples in a glass samples holder. The X-ray diffraction spectra were obtained with a Siemens D-5000 diffractometer, using Cu K α radiation at 40 kV and 30 mA, and a secondary graphite monochromator. The measurements were recorded in steps of 0.02° with a count time of 3 s in the 2 θ range of 5–90°.

3.3. TPD-NH₃

Samples were heated at 400 °C under N₂ flow during 1 h, then cooled to room temperature and saturated with NH₃ (30 cc/min). The excess of ammonia was flushed out with N₂ flow during 30 min. Ammonia desorption was accomplished by increasing the temperature at 10 °C/min until 500 °C. An Altamira AMI-3 automated instrument operating in the programmed thermodesorption mode was used.

3.4. FTIR-pyridine adsorption

Transparent pellets of the oxides were put in a stainless steel sample holder with CaF₂ windows, which allows vacuum in situ and thermal treatments. The samples was desorbed at 400 °C during 2 h and then cooled to room temperature. After, pyridine was introduced in to the cell and it was maintained in contact with the sample for 30 min. The excess of pyridine was eliminated in vacuum and pyridine desorption was accomplished by heating from room temperature to 400 °C. The spectra were obtained with a 710SX Nicolet FTIR spectrometer.

3.5. FTIR-CO₂ adsorption

After desorption at 400 °C, the sample was cooled to –100 °C using liquid nitrogen. Then CO₂ (30 Torr) was admitted into the cell. After 15 min in contact with the sample, the excess of CO₂ was evacuated and the spectra were obtained with a 710SX Nicolet FTIR spectrometer.

3.6. Catalytic activity

The decomposition of isopropanol (Baker, 99%) was determined in a continuous flow reactor (5 ml) at low conversion. The reaction conditions were: catalyst mass 50 mg, isopropanol partial pressure 100 Torr, reaction temperature 150 °C, flow carrier nitrogen (1.8 l/h). The reaction products propene, acetone and isopropylether were analyzed with a VARIAN Star 3600CX gas chromatograph apparatus coupled to the reactant system.

Table 2

Specific surface area and mean pore size diameter of sol–gel TiO₂, ZrO₂, and TiO₂–ZrO₂ mixed oxides annealed at 400 °C

| Catalysts | BET area (m ² /g) | Pore size diameter (Å) |
|--|------------------------------|------------------------|
| TiO ₂ (100) | 110 | 71 |
| TiO ₂ –ZrO ₂ (90–10) | 153 | 52 |
| TiO ₂ –ZrO ₂ (50–50) | 244 | 23 |
| TiO ₂ –ZrO ₂ (10–90) | 128 | 44 |
| ZrO ₂ (100) | 157 | 60 |

4. Results and discussion

4.1. Specific surface areas

The specific surface areas of the isolated oxides and mixed oxides are reported in Table 2. For TiO₂ and ZrO₂ the corresponding specific surface areas were 110 and 157 m²/g, respectively. In mixed oxides the BET specific surface areas varies in depending of the ZrO₂ content, they were 153 (90:10), 244 (50:50) and 128 m²/g (10:90). The largest area was obtained in the mixed oxide showing an amorphous form, as observed by XRD, Fig. 1. In depending of the hydrolysis-condensation rate of the titanium or zirconium alkoxides the particle agglomeration behavior could be affected and the different textural properties of the mixed oxides are a result of such effects. In example, the mean pore size diameter calculated with the BJH method corresponds in all the solids to mesoporous materials (23–71). As an effect of the competitive hydrolysis reactions the small pore diameter was obtained in the mixed oxides.

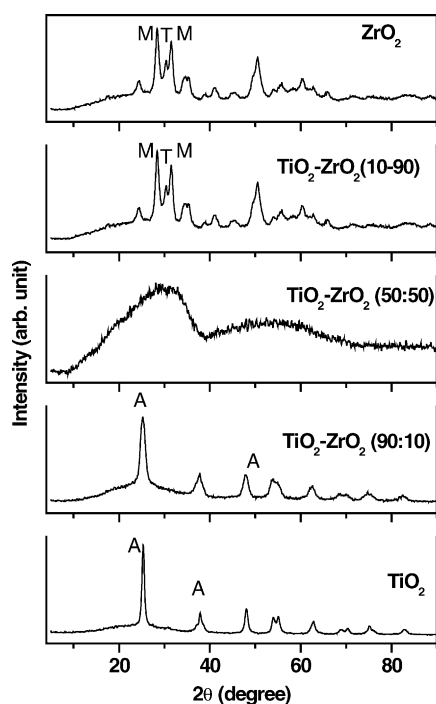


Fig. 1. XRD pattern of TiO₂, ZrO₂ and TiO₂–ZrO₂ mixed oxides annealed at 400 °C.

4.2. XRD diffraction

XRD pattern for annealed samples at 400 °C are shown in Fig. 1. In the TiO₂ spectrum the peak at $\theta = 25.5$ corresponds to the anatase crystalline phase with a crystallite size of 13 nm. In mixed oxides, in the TiO₂ rich region anatase phase is observed with a crystallite size of 13 nm, while in TiO₂–ZrO₂ (50–50) the sample is amorphous. Finally in the ZrO₂ rich region and pure ZrO₂, tetragonal (t) and monoclinic (m) crystalline phases were observed [21–25]. The crystallite size for ZrO₂ was 9 and 11 nm for (t) and (m) phases, respectively. In samples annealed at 400 °C, for TiO₂ rich region crystalline zirconia phases are not observed, while for the ZrO₂ rich region the inverse phenomenon occurs i.e., crystalline titania phases are not observed. In both cases an inhibiting crystallite size growth effect by Zr⁴⁺ or Ti⁴⁺ in TiO₂ and ZrO₂, respectively, may occur [26]. The oxide at low content will be found as a large dispersed oxide in the ZrO₂ or TiO₂ structure, respectively. We can expect that in such cases the crystallite size of the doping oxide will be lower than 5 nm and not observable by XRD. In the TiO₂–ZrO₂ (50–50) sample amorphous material is obtained. According to Tanabe hypothesis [27] models I and II could be the structures of TiO₂–ZrO₂ mixed oxides, where TiO₂ or ZrO₂ are the major component, while the model III will correspond to the 1:1 mixed oxide composition. The hydroxylated form is expected to show an amorphous structure [28], as it can be observed in the XRD pattern of Fig. 1.

4.3. Ammonia thermodesorption

TPD-ammonia thermograms shown a flat and broad NH₃ desorption curve for pure TiO₂ and ZrO₂ (Fig. 2), indicating that such solids have a broad acid sites distribution. The maximum desorption peak for ZrO₂ is observed around 182 °C, whereas for TiO₂ the maximum is around 310 °C. On the other hand, the desorption curves corresponding to the TiO₂–ZrO₂ mixed oxides are characteristic of solids having sharp acid sites distribution. For the TiO₂–ZrO₂ (50–50 and 90–10) samples the maximum temperature desorption peak are around 176 °C, while for the TiO₂–ZrO₂ (10–90) the peak is around 204 °C. The number of acid sites was calculated from the ammonia thermodesorption curves and the values are reported in Table 3. A notable increase in the number of acid sites can be observed in the mixed oxides if they are compared with titania or zirconia. Values of 1326, 1456 and 1226 $\mu\text{mol NH}_3/\text{g}$ corresponding, respectively, to the 90–10, 50–50 and 10–90 TiO₂–ZrO₂ mixed oxides are reported. For titania and zirconia the number of acid sites were 173 and 138 $\mu\text{mol NH}_3/\text{g}$ respectively. Such results clearly indicate that in the mixed oxides a big number of acid sites were developed, suggesting the formation of a great number of acids sites probably due to the substitution of some titanium by zirconium atoms, or by the effect of large dispersion of TiO₂ or ZrO₂ on the surface of the mixed

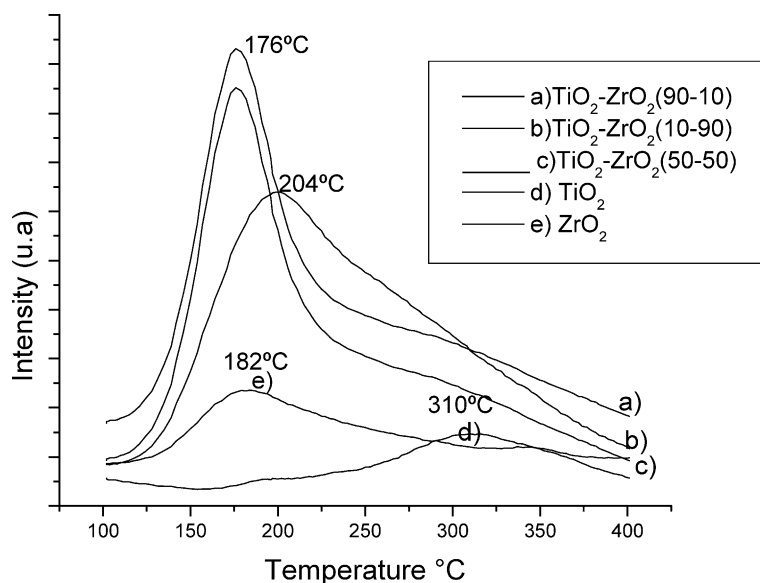


Fig. 2. Ammonia TPD profiles for TiO_2 , ZrO_2 and TiO_2 - ZrO_2 mixed oxides.

oxide. Concerning the strength of the acid sites, usually is accepted that desorption temperature can be related to the strength of the sites. In the mixed oxides the maximum desorption temperature for the TiO_2 - ZrO_2 are found between 176 and 204 °C, while for zirconia and titania they are around 182 and 310 °C, respectively. With exception of TiO_2 we can say that the strength of the acid sites is of the same order. The number of them is which notably differs in the mixed oxides. Moreover from these results, we can speculate about the absence of Brönsted sites, since it has been reported that to Brönsted sites correspond desorption temperatures higher than 400 °C, which is not the case in our catalysts [29,30].

4.4. FTIR-pyridine adsorption

Pyridine adsorption is a valuable method to determine the nature of acid sites. Absorption bands around 1605, 1575, 1490 and 1444 cm^{-1} characteristic of Lewis acid sites [31] can be observed for TiO_2 , ZrO_2 and TiO_2 - ZrO_2 mixed oxides. Brönsted acidity (1540 cm^{-1} band) is not observed in any of the samples, isolated or mixed oxides. In Fig. 3. FTIR-pyridine adsorption spectra for TiO_2 - ZrO_2 90–10,

50–50 and 10–90 wt.% are shown. The adsorption spectra shown that pyridine is not totally desorbed at temperatures of 400 °C. The results also show that acid sites strength in such samples is comparable between them. The number of acid sites determined from pyridine adsorption is reported in Fig. 4. It can be seen that the samples showing the higher number of acid sites correspond to the mixed oxides. Such results confirm that obtained from ammonia thermodesorption, where the isolated TiO_2 and ZrO_2 oxides have the lowest number of acid sites.

4.5. FTIR- CO_2 adsorption

Conventionally to identify basic sites in solids CO_2 adsorption is a recommendable technique. In depending of the basic site strength adsorbed CO_2 was identified as monodentate (1578 and 1359 cm^{-1}) or bidentate carbonates (1672, 1243 and 1053 cm^{-1}) [32,33]. Additionally, absorption bands have been reported at 1630, 1430, 1408 and 1221 cm^{-1} assigned to bicarbonates formed by the interaction between OH groups and CO_2 . In particular for TiO_2 a band at 2338 cm^{-1} is observed and assigned to CO_2 linearly adsorbed on the Ti^{4+} ions [34].

In Fig. 5a, for TiO_2 it can be observed the absorption bands at 1670 and 1600 cm^{-1} corresponding to CO_2 adsorbed on basic sites. On the other hand, in TiO_2 - ZrO_2 (90–10) and 10–90 mixed oxides additional bands at 1539, 1441 and 1250 cm^{-1} for the former and at 1612, 1565, 1363, 1357 and 1259 cm^{-1} for the latter can be observed (Fig. 5b and c), respectively. These bands suggest the creation of new basic sites by the incorporation of ZrO_2 into the TiO_2 . However, in the 50–50 mixed oxide the spectra (not shown) only the absorption bands at 1284 and 1268 cm^{-1} assigned

Table 3
Ammonia adsorption on TiO_2 , ZrO_2 , and TiO_2 - ZrO_2 mixed oxides

| Catalysts | $\mu\text{mol NH}_3/\text{g}$ | $\mu\text{mol}/\text{m}^2$ |
|---|-------------------------------|----------------------------|
| TiO_2 (100) | 173 | 1.57 |
| TiO_2 - ZrO_2 (90–10) | 1326 | 8.67 |
| TiO_2 - ZrO_2 (50–50) | 1456 | 5.97 |
| TiO_2 - ZrO_2 (10–90) | 1226 | 9.58 |
| ZrO_2 | 138 | 0.88 |

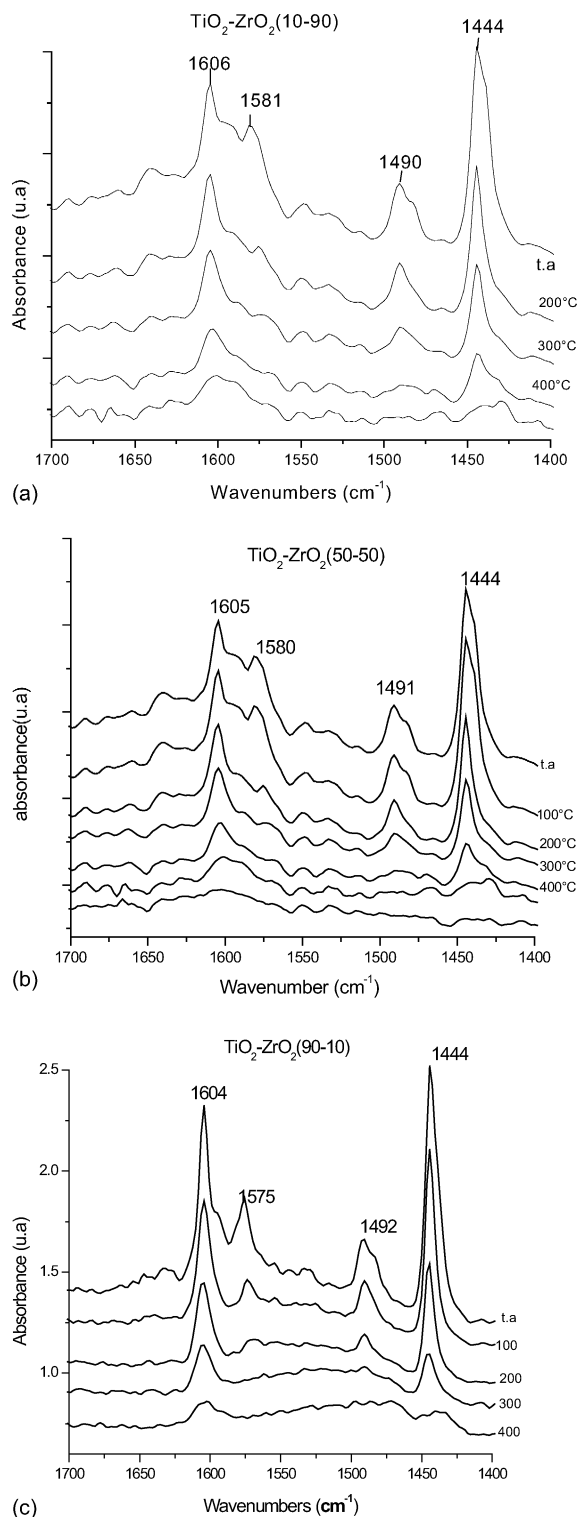


Fig. 3. FTIR-pyridine adsorption on: (a) $\text{TiO}_2\text{-ZrO}_2$ (10–90), (b) $\text{TiO}_2\text{-ZrO}_2$ (50–50) and (c) $\text{TiO}_2\text{-ZrO}_2$ (90–10) thermally annealed at 400°C .

to the interaction between CO_2 and basic OH groups of the solid were observed.

Note that the band at 2338cm^{-1} is observed in the $\text{TiO}_2\text{-ZrO}_2$ mixed oxides (Fig. 5b and c). As established before this band corresponds to CO_2 linearly adsorbed on

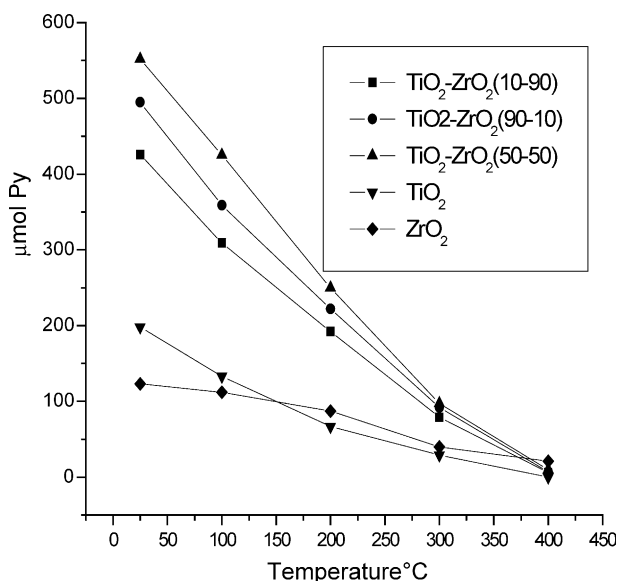


Fig. 4. Pyridine ($\mu\text{mol/g}$) adsorption on TiO_2 , ZrO_2 and $\text{TiO}_2\text{-ZrO}_2$ sol-gel samples annealed at 400°C .

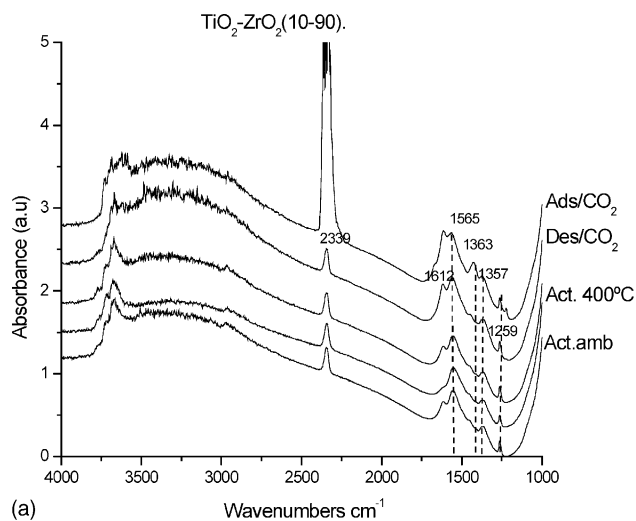
Ti^{4+} ions. The band appears after annealing the sample at 400°C , and resists vacuum desorption, i.e. the samples adsorb CO_2 from the ambient and its intensity does not evolve after CO_2 exposure.

It has been reported that in ZrO_2 strong CO_2 adsorption occurs. In monoclinic zirconia the CO_2 adsorption corresponds to carbonates (1600 and 1430cm^{-1}). On the other hand in tetragonal ZrO_2 the CO_2 adsorption can be as bidentate form (1672 , 1243 and 1053cm^{-1}) [35]. The CO_2 absorption spectrum on ZrO_2 is shown in Fig. 6. Absorption bands assigned to monoclinic zirconia crystalline phase are observed. Note that the CO_2 absorption assigned to tetragonal phase are not present. X-ray diffraction, however, identify the corresponding peaks to both monoclinic and tetragonal zirconia crystalline phase. The absence of CO_2 absorption bands identifying basic sites in tetragonal phase suggested that in mixture of (t) and (m) phases, the CO_2 absorption is selective to basic sites on (m) phases. The intensity of these bands confirms the basic properties of ZrO_2 .

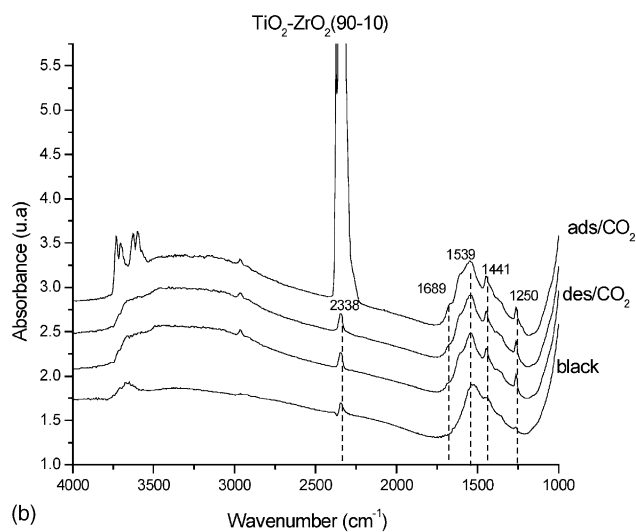
In Fig. 7 [36], the CO_2 coordination is illustrated. When CO_2 is unidentate coordinated this type of sites correspond to strong basic sites (I). In bidentate coordination sites correspond to medium basic strength (II). Finally if CO_2 is coordinated like carbonate this adsorption is assigned to weak basic sites (III). From Fig. 6, we can observe that the mixed oxides have in large proportion medium basic sites.

5. Catalytic activity

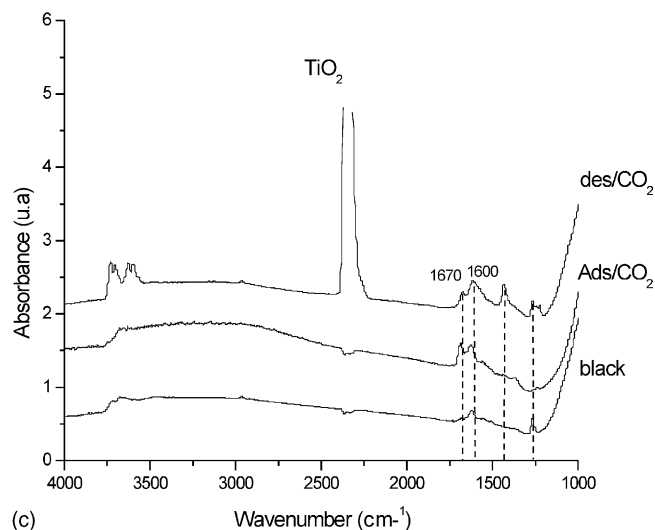
The isopropanol decomposition has been extensively reported as a valuable catalytic test to analyze the acid–basic properties of heterogeneous catalysts [37,38]. Different



(a)



(b)



(c)

Fig. 5. FTIR-CO₂ adsorption on: (a) TiO₂-ZrO₂ (10–90), (b) TiO₂-ZrO₂ (90–10), (c) TiO₂, annealed at 400 °C.

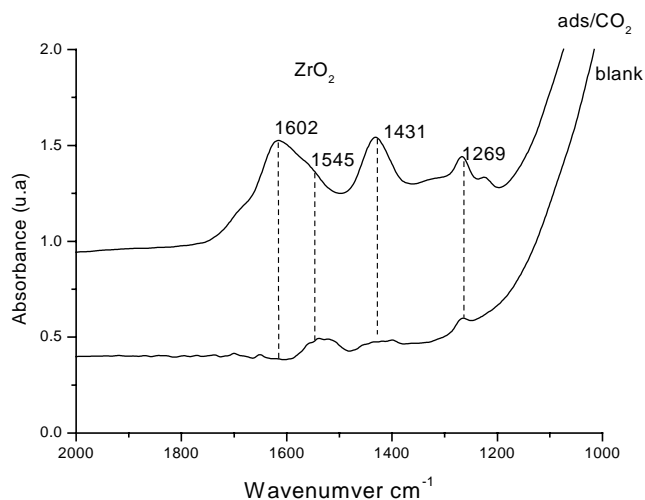


Fig. 6. FTIR-CO₂ adsorption on ZrO₂.

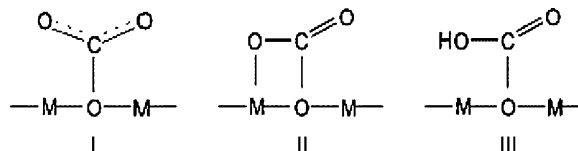


Fig. 7. CO₂ coordination on basic sites: (I) monodentate, (II) bidentate and (III) carbonate.

mechanisms have been reported to explain the role of acid and basic sites in the isopropanol decomposition giving as main products the olefin, acetone and isopropylether. In general is conventionally accepted that acid sites are the responsible for the dehydration activity giving propene. A mechanism is suggested for the dehydration reaction in Fig. 8b, where strong acid sites and weak basic sites are involved. In similar way the formation of the dehydrogenated product (acetone) acid and basic sites are required (Fig. 8a). However, in this case acid sites with moderate strength and strong basic sites are required. On the other hand, for the formation of the ether only acid sites of moderated strength are involved (Fig. 8c). The formation of isopropylether depends then of the number of acid sites preferentially than their strength [39]. In Table 4, the activity

Table 4

Activity and selectivity for the isopropanol decomposition on TiO₂, ZrO₂ and TiO₂-ZrO₂

| Catalyst | R_a ($\times 10^6$ mol/s g) | X_a | Selectivity (%) | | |
|---|-----------------------------------|-------|-----------------|---------|----------------|
| | | | Propene | Acetone | Isopropylether |
| TiO ₂ (100) | 3.01 | 4.67 | 53 | 26 | 22 |
| TiO ₂ -ZrO ₂ (90–10) | 2.16 | 3.35 | 51 | 19 | 31 |
| TiO ₂ -ZrO ₂ (50–50) | 0.85 | 1.32 | 30 | 18 | 53 |
| TiO ₂ -ZrO ₂ (10–90) | 2.27 | 3.52 | 48 | 16 | 36 |
| ZrO ₂ (100) | 2.9 | 4.54 | 46 | 34 | 20 |

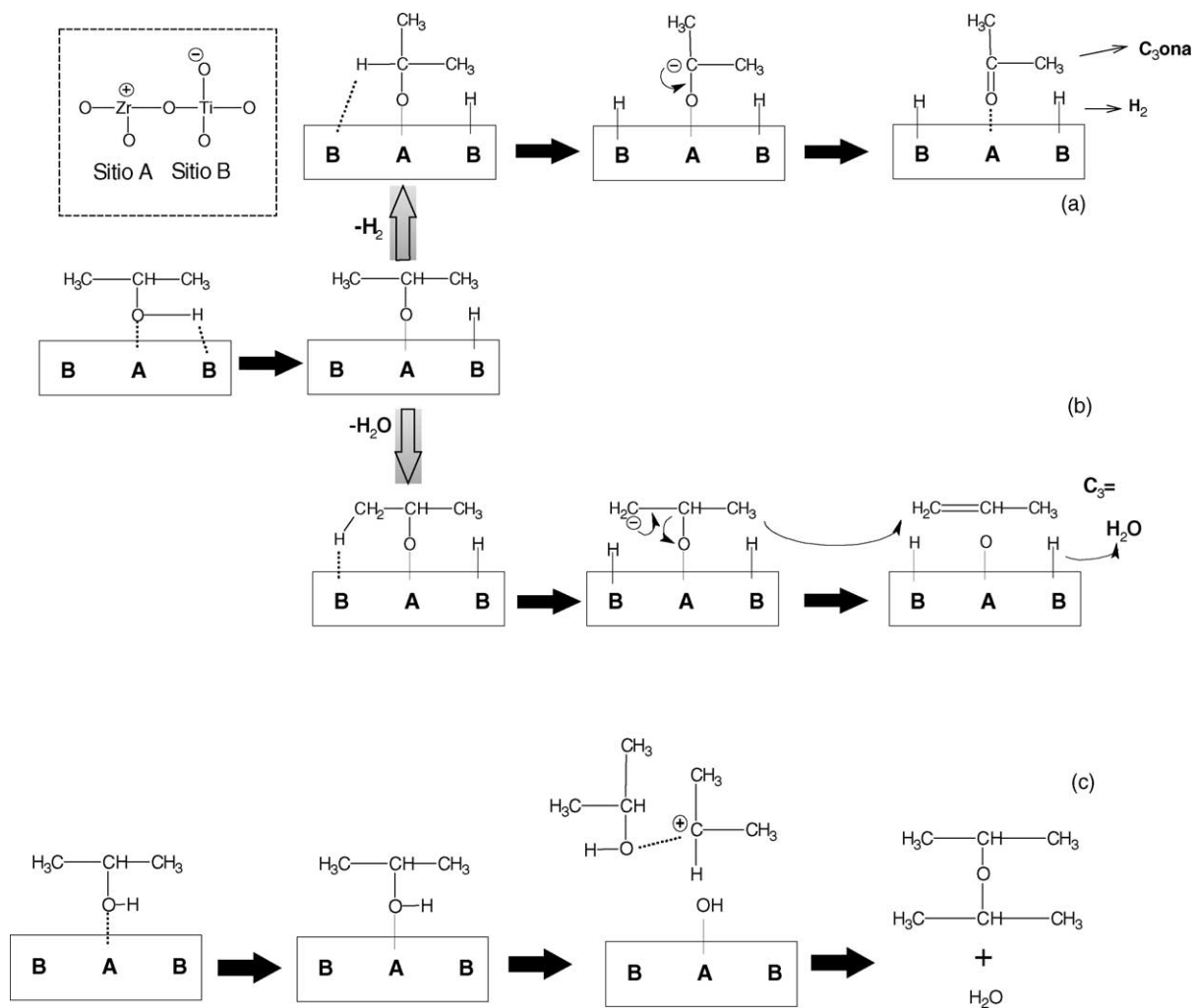


Fig. 8. Mechanisms proposed for the 2-propanol decomposition.

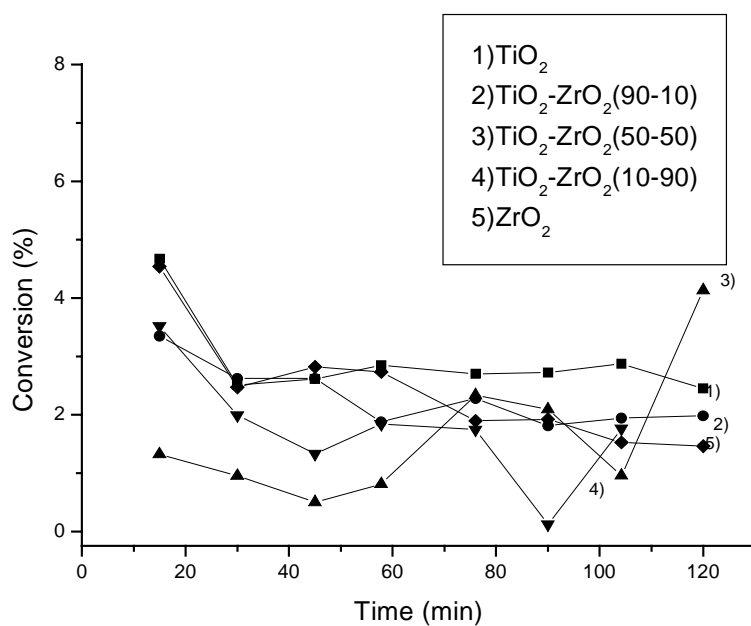


Fig. 9. Isopropanol decomposition in function of time for TiO₂, ZrO₂, and TiO₂-ZrO₂ mixed oxides.

and selectivity for isopropanol decomposition are reported. It can be seen that the conversion of isopropanol is almost of the same order for all the catalysts (<5%), then we have differential reactor conditions. Only a moderated deactivation was observed in these conditions and is of the same order in all catalysts (Fig. 9), then the effects in selectivity will not be discussed in terms of deactivation side reactions.

In Table 4, we can see that the highest selectivity to propene (53%) corresponds to the TiO₂ catalyst, to which also corresponds the ammonia desorption peak at highest temperature. However, it cannot be possible to establish a correlation between the number of acid sites or the ammonia desorption temperature peaks for all of them are in agreement with the results previously reported in this reaction [9]. Concerning the formation of acetone the catalyst showing the highest selectivity was pure ZrO₂ (34%). This result confirms the basic character given to ZrO₂. In TiO₂–ZrO₂ mixed oxides, the formation of acetone is of the same order in all of them 18, 16, and 16% for the 90–10, 50–50 and 10–90 TiO₂–ZrO₂ solids, respectively.

For isopropylether formation, in TiO₂ and ZrO₂ the selectivity is of the same order in both catalysts 22 and 20%, respectively. In Table 3, we can see that the number of acid sites is the lowest in both oxides 173 and 138 μmol NH₃/g, respectively. The ether formation, however, is the higher in the mixed oxides (31–53%), if compared with TiO₂ or ZrO₂. In Tables 3 and 4, it can be seen that the ether formation and the number of acid sites follow a similar sequence. For 1326, 1456, and 1226 μmol NH₃/g acid sites concentration the selectivity was 31, 53 and 36%, respectively. Mixed oxides also show the highest acid site density (8.6, 5.9 and 9.5 μmol NH₃/m²) in TiO₂ and ZrO₂ the density was 1.5 and 0.88 μmol NH₃/m². The agreement with the number but not with the strength (NH₃-TPD) of the acid sites and the selectivity to isopropylether is a good support for the proposed mechanism represented in Fig. 8. The big number of acid sites obtained in the TiO₂–ZrO₂ mixed oxides prepared by the co-gelling of the respective alkoxides, is a result confirming that in both oxides a large number of new acid centers were generated.

6. Conclusions

In the preparation of TiO₂, ZrO₂ and TiO₂–ZrO₂ mixed oxides by co-gelling the corresponding alkoxides, solids with high specific surface were obtained. Acidity determined by NH₃-TPD and FTIR-pyridine adsorption showed that in mixed oxides the number of acid sites is notably increased, pyridine adsorption identify Lewis acid sites. By FTIR-CO₂ the formation of monodentate and bidentate carbonates were identified. Thus in this catalysts acid and basic sites co-exist. XRD spectra of samples treated at 400 °C shows anatase as the predominant crystalline phase in TiO₂ and in the rich TiO₂ mixed oxide (90–10). In the mixed oxide at 50–50 composition the sample is almost amorphous. On the other

hand in the ZrO₂ rich sample (10–90) and pure ZrO₂ a mixture of tetragonal and monoclinic crystalline phases were observed. Activity in the isopropanol decomposition is of the same order for all the catalysts. Nevertheless, selectivity to propene, acetone and isopropylether varies in function of the acid–basic properties. In mixed oxides is obtained the great amount of isopropylether. The selectivity is found as a function of the number of acid sites (mainly density than strength of them). These results showed that by the sol–gel method it is possible to prepare catalysts with controlled selectivity to propene, acetone or isopropylether in depending of the relative amounts of TiO₂ and ZrO₂ in the mixed oxides.

Acknowledgements

We acknowledge to the Conacyt by the support giving to this study. M.E. Manríquez by the scholarship RE-111634.

References

- [1] J.A. Linnekoski, A.O.I. Krause, A. Holmen, M. Kjetsa, K. Moljord, *Appl. Catal. A Gen.* 174 (1998) 1.
- [2] L. de Mourges, F. Peyron, Y. Trambouze, M. Prettre, *J. Catal.* 7 (1967) 117.
- [3] A. Corma, V. Fornés, F. Rey, *J. Catal.* 148 (1994) 205.
- [4] A.A. Aramendía, V. Borau, C. Jiménez, J.M. Marinas, A. Porras, F.J. Urbano, *React. Kinet. Catal. Lett.* 53 (1994) 397.
- [5] P. Berteau, B. Delmon, *Appl. Catal.* 70 (1991) 307.
- [6] P. Berteau, S. Ceckiewicz, B. Delmon, *Appl. Catal.* 31 (1987) 361.
- [7] M.G. Cutrufello, I. Ferino, V. Solinas, A. Primavera, A. Trovarelli, A. Auroux, C. Picciau, *J. Phys. Chem.* 1 (1999) 3369.
- [8] A. Auroux, P. Artizzi, I. Ferino, R. Monaci, E. Rombi, V. Solinas, *Micropor. Mater.* 11 (1997) 117.
- [9] J.A. Wang, X. Bokhimi, O. Novaro, T. López, F. Tzompantzi, R. Gómez, J. Navarrete, M.E. Llanos, E. López-Salinas, *J. Mol. Catal. A Chem.* 137 (1999) 239.
- [10] R. Valarivan, C.N. Pillai, C.S. Swamy, *React. Kinet. Catal. Lett.* 53 (1994) 429.
- [11] M.A. Aramendía, V. Boáu, I.M. García, C. Jiménez, A. Marinas, J.M. Marinas, A. Porras, F.J. Urbano, *Appl. Catal. A* 184 (1999) 115.
- [12] K. Arata, H. Sawamura, *Bull. Chem. Soc. Jpn.* 48 (1975) 3377.
- [13] H. Knözinger, H. Büll, K. Kochloeff, *J. Catal.* 24 (1972) 57.
- [14] H. Közinger, A. Schengllia, *J. Catal.* 33 (1974) 142.
- [15] N. Satoh, J.I. Hayashi, H. Hattori, *Appl. Catal. A Gen.* 202 (2000) 207.
- [16] G. Cai, Z. Lin, R. Shi, C. He, L. Yang, C. Sun, Y. Chang, *Appl. Catal. A Gen.* 125 (1995) 29.
- [17] J.A. Wang, X. Bokhimi, O. Novaro, T. López, R. Gómez, *J. Mol. Catal. A Chem.* 145 (1999) 291.
- [18] T. López, R. Gómez, J. Navarrete, E. López-Salinas, *J. Sol–Gel Sci. Technol.* 13 (1998) 1043.
- [19] T. López, M.E. Manríquez, R. Gómez, A. Campero, M.E. Llanos, *Mater. Lett.* 46 (2000) 21.
- [20] J.P. Dalmon, D. Bernard, J.M. Bonnier, *Farad. Trans. I* 70 (1974) 2021.
- [21] H. Matsuhashi, M. Hinio, K. Arata, *Appl. Catal.* 59 (1990) 203.
- [22] T. Lopez, M.E. Manríquez, R. Gomez, X. Bokhimi, *J. Solid State Chem.* (in press).
- [23] D. Das, H.K. Mishra, A.K. Dalai, K.M. Parida, *Appl. Catal. A Gen.* 243 (2003) 271.

- [24] M.E. Manríquez, T. López, D.H. Aguilar, P. Quintana, in: T. Lopez, D. Avnir, M. Aegerter (Eds.), *Emerging Fields in Sol–Gel Science and Technology Materials*, Kluwer Academic Publishers, 2003, p. 254.
- [25] J.A. Wang, O. Novaro, X. Bokhimi, T. Lopez, R. Gómez, *J. Phys. Chem. B* 105 (2001) 9692.
- [26] Y.M. Wang, S.W. Liu, M.K. Lu, S.F. Wang, F. Gu, X.Z. Gai, X.P. Cui, J. Pan, *J. Mol. Catal. A Chem.* 215 (2004) 137.
- [27] K. Tanabe, T. Sumiyoshi, K. Shibata, *Bull. Chem. Soc. Jpn.* 47 (1974) 1064.
- [28] I. Wang, W. Chang, R. Shiau, J. Wu, C. Chung, *J. Catal.* 83 (1983) 428.
- [29] H. Zou, Y.S. Lin, *Appl. Catal. A Gen.* 265 (2004) 35.
- [30] D. Das, H.K. Mishra, A.K. Dalai, K.M. Parida, *Appl. Catal. A Gen.* 243 (2003) 271.
- [31] R. Barthos, F. Lónyi, J. Engelhardt, J. Valyon, *Top. Catal.* 10 (2000) 79.
- [32] D.J. Suh, T.J. Park, *Chem. Mater.* 14 (2002) 1452.
- [33] G. Martra, *Appl. Catal. A Gen.* 200 (2000) 275.
- [34] M.A. Aramendía, V. Borau, C. Jiménez, J.M. Marinas, J.R. Ruiz, F.J. Urbano, *Appl. Catal. A Gen.* 244 (2003) 207.
- [35] K. PoKrovski, K.T. Jung, A.T. Bell, *Langmuir* 17 (2001) 4297.
- [36] M.A. Aramendía, V. Borau, C. Jiménez, J.M. Marinas, J.R. Ruiz, F.J. Urbano, *Appl. Catal. A Gen.* 244 (2003) 207–215.
- [37] B. Shi, B.H. Davis, *J. Catal.* 157 (1995) 359.
- [38] V.K. Díez, C.R. Apesteguía, J.I. Di Cosimo, *Catal. Today* 63 (2000) 53.
- [39] P. Berteau, M. Ruwet, B. Delmon, *Bull. Soc. Chim. Belg.* 94 (1985) 11.